Structural basis for the differential interaction of Scribble PDZ domains with the guanine nucleotide exchange factor β-PIX

Received for publication, May 28, 2017, and in revised form, October 11, 2017 Published, Papers in Press, October 23, 2017, DOI 10.1074/jbc.M117.799452

Krystle Y. B. Lim[‡§], **Nathan J. Gödde**[‡§], **Patrick O. Humbert**[‡§¶‖**1], **and Marc Kvansakul**[‡2]

From the [‡]*Department of Biochemistry and Genetics, La Trobe Institute for Molecular Science, La Trobe University, Melbourne, Victoria 3086, the* [§]*Cell Cycle and Cancer Genetics Laboratory, Research Division, Peter MacCallum Cancer Centre, Melbourne, Victoria 3002, the* [¶]*Sir Peter MacCallum Department of Oncology, University of Melbourne, Melbourne, Victoria 3002, and the Departments of* [‖]*Biochemistry and Molecular Biology and* **Pathology, *University of Melbourne, Melbourne, Victoria 3010, Australia*

Edited by Eric R. Fearon

Scribble is a highly conserved protein regulator of cell polarity that has been demonstrated to function as a tumor suppressor or, conversely, as an oncogene in a context-dependent manner, and it also controls many physiological processes ranging from immunity to memory. Scribble consists of a leucine-rich repeat domain and four PDZ domains, with the latter being responsible for most of Scribble's complex formation with other proteins. Given the similarities of the Scribble PDZ domain sequences in their binding grooves, it is common for these domains to show overlapping preferences for the same ligand. Yet, Scribble PDZ domains can still exhibit unique binding profiles toward other ligands. This raises the fundamental question as to how these PDZ domains discriminate ligands and exert specificities in Scribble complex formation. To better understand how Scribble PDZ domains direct cell polarity signaling, we investigated here their interactions with the well-characterized Scribble binding partner β-PIX, a guanine nucleotide exchange factor. We report the interaction profiles of all isolated Scribble PDZ domains with a β-PIX peptide. We show that Scribble PDZ1 and PDZ3 are the major interactors with β-PIX and reveal a distinct binding hierarchy in the interactions between the individual Scribble PDZ domains and β-PIX. Furthermore, using crystal structures of PDZ1 and PDZ3 bound to β-PIX, we define the structural basis for Scribble's ability to specifically engage β-PIX via its PDZ domains and provide a mechanistic platform for understanding Scribble-β-PIX–coordinated cellular functions such as directional cell migration.

Cell polarity is an essential property of eukaryotic cells and is critical for tissue development and correct tissue architecture. At the molecular level, cell polarity results in the asymmetric distribution of proteins, lipids, and carbohydrates into distinct cellular domains (1). This uneven distribution of cellular contents in epithelial cells gives rise to apical–basal cell polarity, which is important for the regulation of crucial cellular signaling pathways, including those associated with apoptosis, vesicle trafficking, cell proliferation, and migration (2). Conversely, loss of cell polarity is an important hallmark of cancer development (3).

Scribble, a key regulator of cell polarity, is part of the Scribble module comprising Scribble, Dlg, and Lgl, which in conjunction with the Par and Crumbs complex controls apical–basal polarity (4–6). Scribble was initially discovered in *Drosophila melanogaster* as a tumor suppressor where Scribble loss disrupts epithelial organization and causes aberrant growth in the imaginal discs of the larvae (7). This tumor-suppressing activity is conserved across species, and in mouse models, loss of Scribble promotes tumor initiation and, in combination with oncogenic drivers such as RAS, tumor progression in multiple epithelial tissue types, including mammary, prostate, skin, and the lung (8–12). As Scribble localization is spatially restricted in most cell types, Scribble has been postulated to act as a site-specific adaptor protein that mediates molecular interactions and in particular functions to direct distinct signaling complexes to subcellular sites (4). In disease states such as prostate cancer, mislocalization of Scribble correlates with poor patient prognosis (10), whereas in breast cancer mislocalized Scribble can act as an oncogene to drive tumorigenesis via activation of the Akt/mTOR/S6 kinase pathway (13). Thus, although mislocalization of Scribble may not alter its function *per se*, it is likely to alter the pool of accessible ligands, resulting in aberrant interactions leading to oncogenic signaling (3, 4). In addition to its tumor modulatory activities, Scribble regulates polarity and signaling in a wide number of cell types and organisms, playing a crucial role in organ development and physiology. This includes the development of the cardiovascular system, skeletal muscle stem cells, myelination, skin barrier formation, as well as regulation of physiological responses ranging from mammalian immunity to memory loss in *Drosophila* (4, 9, 14–17). Thus, understanding how Scribble functions has broad implications for understanding a wide number of biological systems.

This work was supported in whole or part by the National Health and Medical Research Council Australia Project Grant APP1103871 (to M. K. and P. O. H.), Senior Research Fellowship APP1079133 (to P. O. H.), Australian Research Council Fellowship FT130101349 (to M. K.), and La Trobe University Scholarship (to K. Y. B. L.). The authors declare that they have no conflicts of interest with the contents of this article.

The atomic coordinates and structure factors (codes 5VWC, 5VWK, and 5VWI) have been deposited in the Protein Data Bank (http://wwpdb.org/).

[1] To whom correspondence may be addressed: Dept. of Biochemistry and Genetics, La Trobe University, Melbourne, Victoria 3086, Australia. Tel.: 61-3-9479-5155; Fax: 61-3-9479-2467; E-mail: p.humbert@latrobe.edu.au.

[2] To whom correspondence may be addressed: Dept. of Biochemistry and Genetics, La Trobe University, Melbourne, Victoria 3086, Australia. Tel.: 61-3-9479-2263; Fax: 61-3-9479-2467; E-mail: m.kvansakul@latrobe.edu.au.

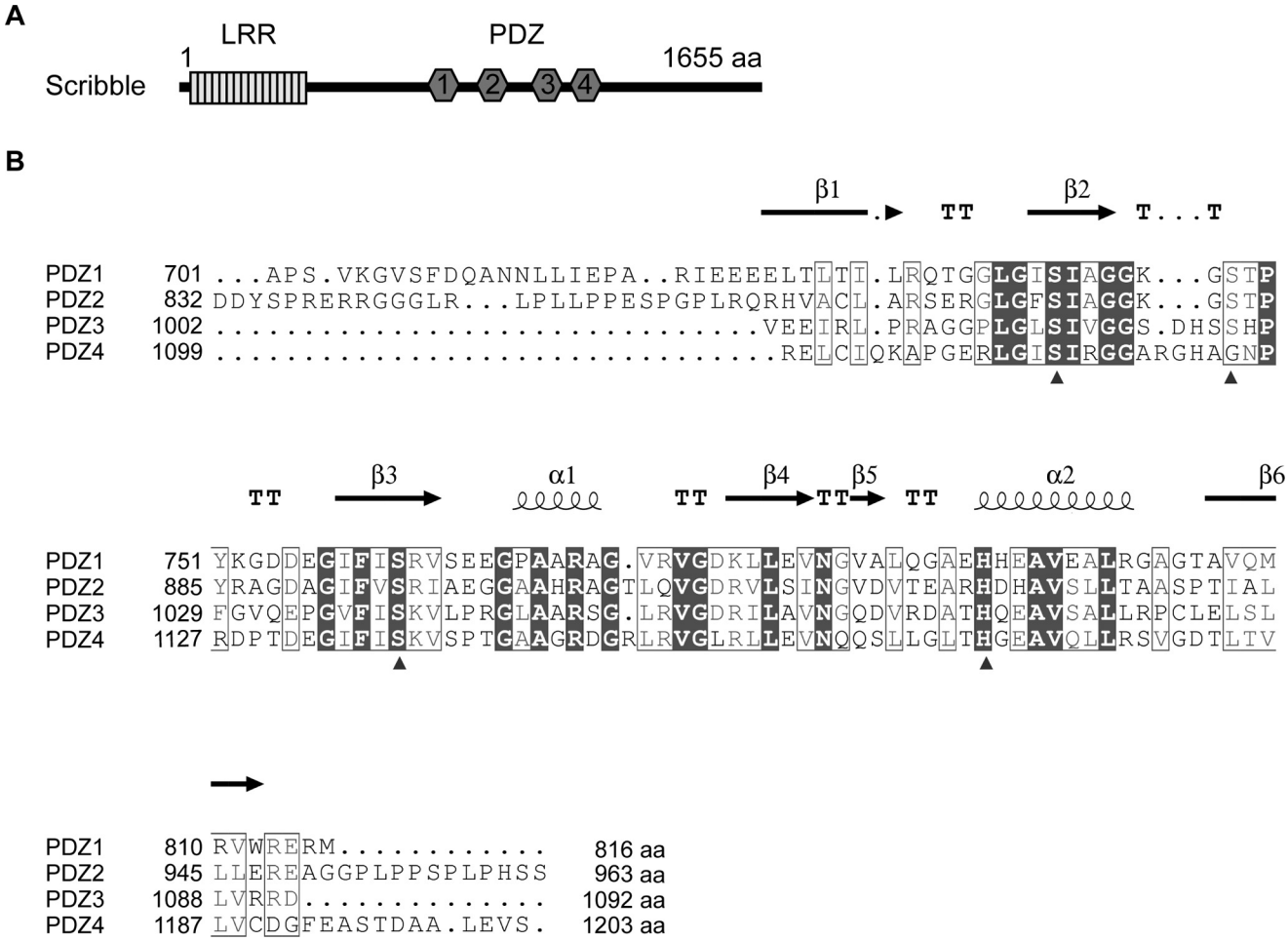

Figure 1. Schematic and sequence alignment of Scribble PDZ domains. *A,* schematic of the Scribble domain structure containing an LRR domain and four PDZ domains. *B,* structure-based sequence alignment of Scribble PDZ domains generated by ESPript (http://espript.ibcp.fr; please note that the JBC is not responsible for the long-term archiving and maintenance of this site or any other third party hosted site) (41) based on the PDZ1 crystal structure. *Boxes* with *white fill* denote similar residues, and *boxes* with *black fill* denote conserved residues across the four PDZ domains. Helices are displayed as *looped lines*; β-strands are denoted as *arrows*; *TT* represents turns. The *arrows* below the aligned sequences represent residues that interact with the β-PIX peptide based on the determined crystal structures. The PDZ domain binding site consists of a "GLGF" motif preceding β2, β2, and α2 residues. *aa,* amino acids.

Scribble includes 16 leucine-rich repeats (LRR)[3] and four PSD-95/Disc-large/ZO-1 (PDZ) domains and belongs to the LAP family of proteins (Fig. 1*A*). These domains enable Scribble interactions with a wide range of ligands that are involved in multiple discrete signaling pathways. For example, the Scribble LRR domain can associate with the Lgl2 protein that is also involved in the regulation of cell polarity (18). During directed cell migration, vimentin interacts with Scribble PDZ domains to regulate its proteasome degradation, allowing Scribble to induce polarization of the Golgi apparatus (19). Scribble is also involved in receptor recycling by binding to thyroid-stimulating hormone receptor and activating ARF6 through the recruitment of a β-PIX–GIT1 complex upon thyroid-stimulating hormone stimulation (20). Again, the majority of these interactions occur through Scribble PDZ domains. All four Scribble PDZ domains share high levels of sequence identity (Fig. 1*B*), raising the question of how specificity for distinct interactions with Scribble ligands is achieved. Notably, the Scribble PDZ domains appear to harbor overlapping preferences for certain ligands, with each PDZ domain capable of engaging multiple binding partners. To understand how Scribble PDZ domains distinguish between ligands and achieve selectivity and specificity, we examined Scribble interactions with a well-established and characterized binding partner, β-PIX. β-PIX is a guanine nucleotide exchange factor for small GTPases, where its membrane-associated localization is dependent on Scribble interaction (21). Scribble and β-PIX complexes are found in various cell types ranging from epithelial and neuronal cells to endothelial cells where they regulate cellular processes such as vesicle trafficking (22), receptor recycling (20), cytoskeletal organization, and cell migration (23–25). Previous studies have shown that all four of Scribble PDZ domains can bind to β-PIX (22, 26). Here, we directly examine the redundancy of Scribble PDZ domain affinity toward β-PIX and investigate the differences in Scribble PDZ domain affinity for β-PIX. To this end, we purified Scribble PDZ domains as four individual domains, and we characterized the interaction of each of the PDZ

[3] The abbreviations used are: LRR, leucine-rich repeat; PBM, PDZ-binding motif; PDB, Protein Data Bank; MBP, maltose-binding protein; BisTris, 2-[bis(2-hydroxyethyl)amino]-2-(hydroxymethyl)propane-1,3-diol; Bistris propane, 1,3-bis[tris(hydroxymethyl)methylamino]propane; r.m.s.d., root mean square deviation.

A

β-PIX peptides

Wild type : P A W D E T N L
Mutant : P A W D E A N A

B

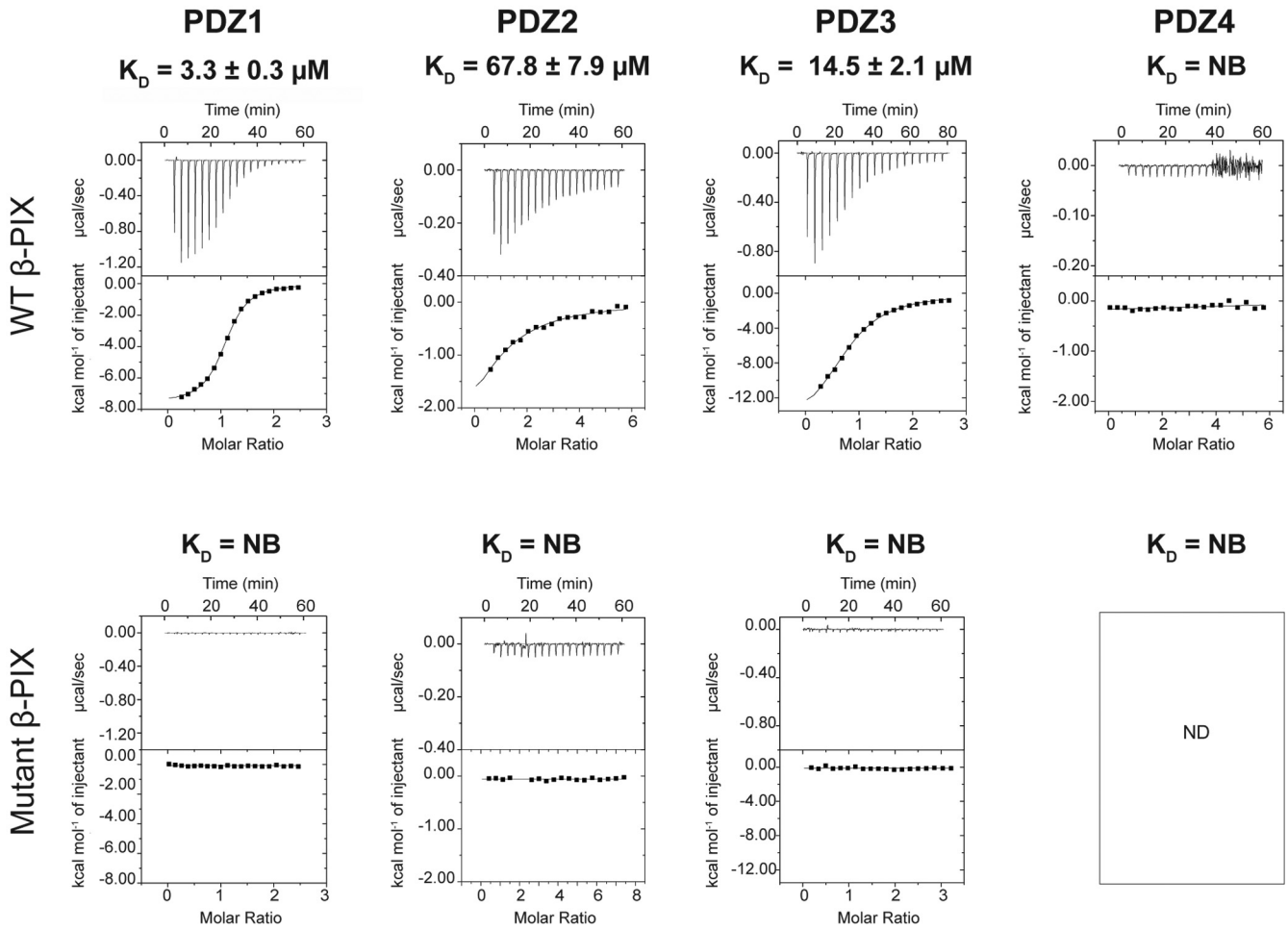

Figure 2. Interaction profiles of Scribble PDZ domains with β-PIX peptides. *A,* sequences of β-PIX peptides used in this study. Both wild-type (*WT*) and mutant peptides sequences are shown, with the altered residues presented as *white font* on *black background*. *B,* binding profiles of isolated Scribble PDZ domain interactions with β-PIX peptides are displayed. Each profile is represented by a raw thermogram (*top panel*) and a binding isotherm fitted with a one-site binding model (*bottom panel*). K_D, dissociation constant; ±, standard deviation; *NB,* no binding. Each of the values was calculated from at least three independent experiments.

domains with a peptide corresponding to the β-PIX C-terminal PDZ-binding motif (PBM). Using isothermal titration calorimetry and pulldown assays, we quantitate and reveal the binding hierarchy for Scribble PDZ domain affinity for β-PIX. Finally, we determined crystal structures of Scribble PDZ1 alone, as well as PDZ1 and PDZ3 in complex with β-PIX peptide. Through these studies, we have identified the specific residues involved in the interaction and propose a model by which Scribble–β-PIX interaction specificity is achieved.

Results

Isolated Scribble PDZ domains specifically interact with the β-PIX PBM

Scribble has previously been shown to directly interact with β-PIX C-terminal PBM using all four of its PDZ domains, with the last three C-terminal amino acids of β-PIX being essential for the interaction (22, 26). However, no comprehensive quantitative affinity measurements for all Scribble PDZ domains were available. To understand how individual Scribble PDZ domains contribute to the interaction with β-PIX, and to determine whether there are functionally relevant differences for interactions between the individual Scribble PDZ domains, we recombinantly expressed and purified all four Scribble PDZ domains and examined their affinity for an 8-mer peptide corresponding to the β-PIX PBM (Fig. 2*A*).

Unexpectedly, we observed marked differences in the interactions between each of the Scribble PDZ domains and β-PIX. Although PDZ domains 1–3 bound to β-PIX with micromolar affinities, we were unable to observe any interaction of PDZ4 with β-PIX. Furthermore, although PDZ1–3 interacted with

A

Superpeptides

Wild type : R S W F E T W V
Mutant : R S W F E A W A

B

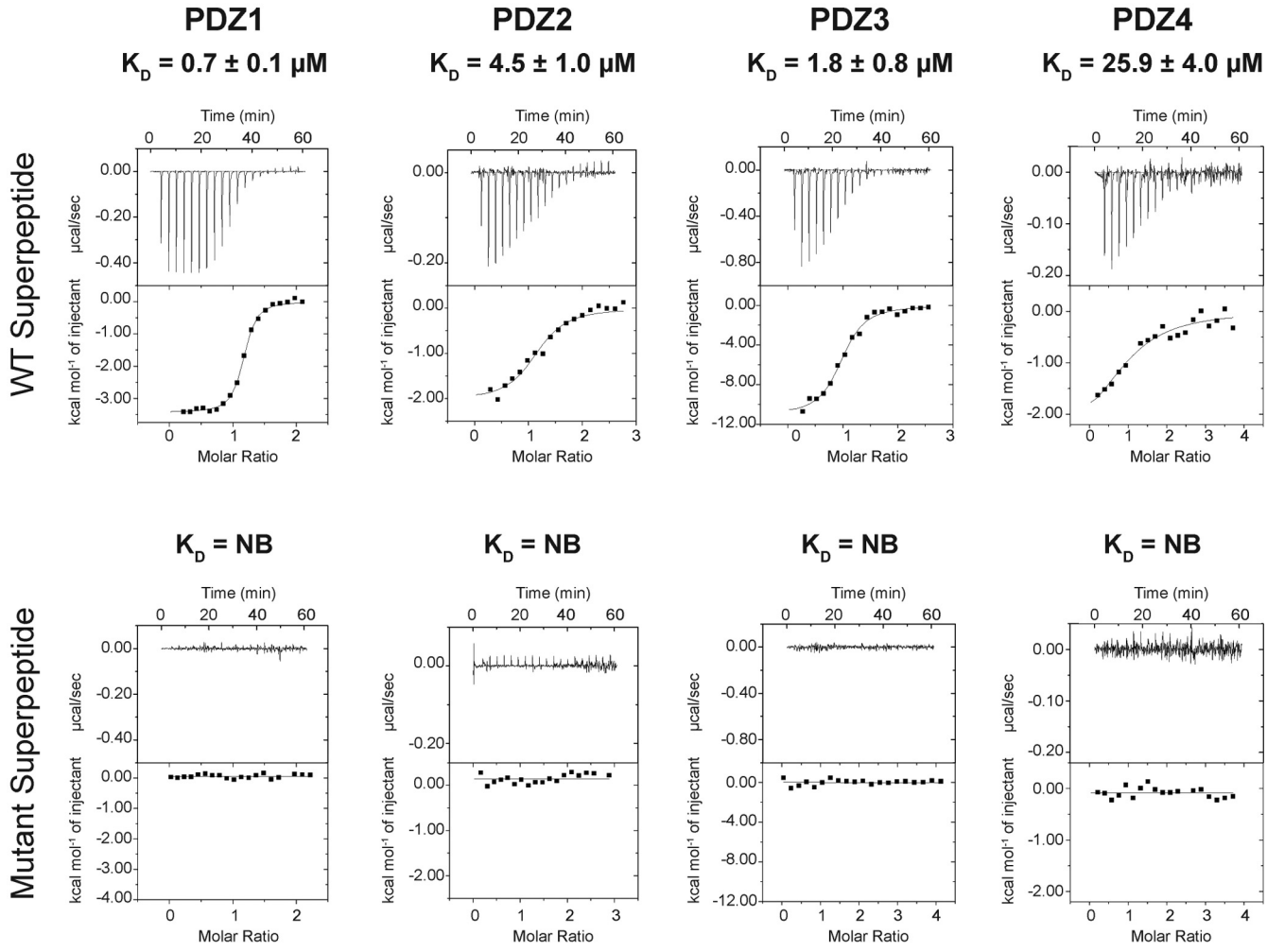

Figure 3. Interaction profiles of Scribble PDZ domains *versus* superpeptides. *A,* wild-type and mutant superpeptides sequences (27) are displayed, with the altered residues shown as *white font* on *black background*. *B,* isothermal titration calorimetry binding profiles of isolated PDZ domain interactions with superpeptides. Each profile is represented by a raw thermogram (*top panel*) and a binding isotherm fitted with a one-site binding model (*bottom panel*). Each binding profile is a representative example from three independent experiments. K_D, dissociation constant; ±, standard deviation; *NB,* no binding. Each of the value was calculated from at least three independent experiments.

β-PIX, substantial differences were detected in the affinities. PDZ1 was identified as the strongest binder at 3.3 μM followed by PDZ3 with 14.5 μM, whereas the interaction with PDZ2 was significantly weaker at 67.8 μM. As expected, PDZ1–4 did not interact with a mutant form of β-PIX where the C-terminal TNL residues were changed to ANA (Fig. 2*B*). To confirm that our recombinant PDZ domains were active and indeed capable of interactions with a given PBM (Fig. 3*B*), we also determined the affinities of PDZ1–4 for a synthetic superpeptide that displays high affinity to a vast pool of PDZ domains and is considered a pan-PDZ-binding peptide (Fig. 3*A*) (27). As expected, all four PDZ domains showed micromolar affinities for the superpeptide, confirming that the lack of interaction of PDZ4 for β-PIX is significant. Together our data demonstrate that PDZ1 has the highest affinity, followed by PDZ3 and PDZ2, thus establishing a binding hierarchy for Scribble PDZ domains and β-PIX C-terminal PBM interaction.

Interaction of isolated PDZ domains with full-length β-PIX

To examine the significance of our observation of a differential β-PIX binding profile among the Scribble PDZ domains in a cellular context, we performed pulldown experiments of individual recombinant GST-PDZ fusion domains with lysates from HEK293T cells that harbor endogenous full-length β-PIX. Consistent with our initial findings, PDZ1 and PDZ3 interacted with endogenous β-PIX (Fig. 4), whereas PDZ4 did not. However, pulldown experiments with PDZ2 did not show detectable amounts of endogenous β-PIX (Fig. 4),

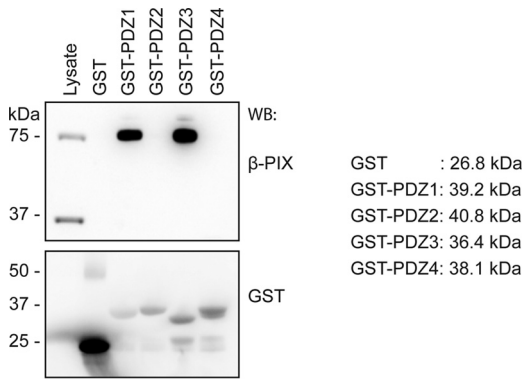

Figure 4. Pulldown assay of individual GST-tagged Scribble PDZ domains against HEK293T cell lysate. GST-tagged isolated Scribble PDZ domains (GST-*X*; *X* represents the number of the PDZ domain) were incubated with HEK293T cell lysates. Glutathione resin was used to capture endogenous full-length β-PIX bound to GST-Scribble PDZ proteins. Captured proteins were analyzed by SDS-PAGE and revealed by Western blotting (*WB*). Data shown are representative from three biological replicates.

suggesting that the K_D of 67.8 μM is too weak to be detected in this setting.

Crystals structures of PDZ1–β-PIX peptide and PDZ3–β-PIX peptide

To understand the structural basis of the differential interactions between Scribble PDZ1–3 domains with the β-PIX peptide, we determined crystal structures of PDZ1 as well as complexes of PDZ1–β-PIX and PDZ3–β-PIX (Figs. 5 and 6). PDZ1 adopts a compact globular fold comprising six β-strands and two α-helices that form a β-sandwich structure, with our determined structure being essentially identical to the previously solved structure (PDB code 2W4F) as indicated by an r.m.s.d. of 0.356 Å over 77 Cα atoms. PDZ1 engages β-PIX using the canonical ligand-binding groove found in PDZ domains that is formed by the β2 strand and helix α2 (Fig. 5*A*). β-PIX is oriented in an anti-parallel manner to the β2 strand, with the C terminus of β-PIX packed against the β1–2 loop. Leu-646$^{\beta\text{-PIX}}$ is located in a hydrophobic pocket formed by PDZ1 Leu-738, Ile-740, Ile-742, Val-797, and Leu-800, whereas Trp-641$^{\beta\text{-PIX}}$ packs against PDZ1 Gly-744 and Tyr-751. In addition, three hydrogen bonds are formed by Asn-645$^{\beta\text{-PIX}}$–Ser-741$^{\text{PDZ1}}$, Glu-643$^{\beta\text{-PIX}}$–Ser-761$^{\text{PDZ1}}$, and Thr-644$^{\beta\text{-PIX}}$–His-793$^{\text{PDZ1}}$ (Fig. 5*E*). Binding of the PBM of β-PIX to PDZ1 does not result in significant changes in the overall PDZ1 structure, with the complex of PDZ1–β-PIX superimposing onto PDZ1 alone with an r.m.s.d. of 0.9 Å over 96 Cα (Fig. 5*D*). The PDZ1–β-PIX complex features a number of crystal contacts that are mediated by a 14-residue segment N-terminal of the PDZ1 domain, and it packs against the loop connecting helix α2 and strand β6 from a neighboring PDZ1 molecule. The β-PIX-binding groove of PDZ1 is oriented toward a solvent channel.

The overall topology of the PDZ3–β-PIX complex is similar to PDZ1–β-PIX (Fig. 5*F*), and the two complexes superimpose with an r.m.s.d. of 1.5 Å over 89 Cα residues (Fig. 5*G*). In the PDZ3–β-PIX structure, the pocket accommodating Leu-646$^{\beta\text{-PIX}}$ is formed by PDZ3 Leu-1014, Leu-1016, Ile-1018, Val-1075, and Leu-1079, and hydrogen bonds are contributed by Asn-645$^{\beta\text{-PIX}}$–Ser-1017$^{\text{PDZ3}}$, Glu-643$^{\beta\text{-PIX}}$–Ser-1039$^{\text{PDZ3}}$, and Thr-644$^{\beta\text{-PIX}}$–His-1071$^{\text{PDZ3}}$ (Fig. 5*F*). Notably, Trp-641$^{\beta\text{-PIX}}$ adopts a different conformation in the PDZ3–β-PIX complex compared with the PDZ1 complex and now contributes a hydrogen bond via Ser-1026$^{\text{PDZ3}}$. The PDZ3–β-PIX complex features a number of crystal contacts, including an interface where the two N-terminal Pro and Ala residues of the β-PIX peptide pack against the β1 strand of a neighboring PDZ3 domain. A second crystal interface is formed by the loop connecting strands β2 and β3, which packs against the β3–α1 loop from a neighboring PDZ3 domain.

Because the major structural differences in β-PIX conformation between the complexes with Scribble PDZ1 and PDZ3 domains are centered on the orientation of Trp-641, we generated a panel of mutations to further examine the role of Trp-641 for the interactions with Scribble PDZ1 and -3 domains (Fig. 7). Mutation of PDZ1 Y751S was predicted to interfere with the packing of β-PIX Trp-641 due to the loss of the aromatic ring, and it resulted in a K_D of 28.2 μM. In contrast, mutation of PDZ3 S1026A led to a modest increase in β-PIX binding (K_D = 9.6 μM), suggesting that this hydrogen bond is not a key contributor to the binding of β-PIX.

Analysis of the configuration of the β2–3 loops that harbor key interaction residues for β-PIX binding in Scribble PDZ1 and -3 revealed that in PDZ1 this loop is shorter and more rigid. Indeed, chimeric PDZ1 with a β2–3 loop from PDZ3 (PDZ1$^{\text{PDZ3LoopRegion}}$) bound β-PIX with a K_D of 44.4 μM, whereas chimeric PDZ3 with a β2–3 loop from PDZ1 (PDZ3$^{\text{PDZ1LoopRegion}}$) bound β-PIX with a K_D of 1 μM, suggesting that the β2–3 loop is a critical regulator of β-PIX binding. To further understand the role of the loop in PDZ-binding specificities, we asked if the length of the loop is a key determining factor for PDZ1 and -3 binding to β-PIX. We generated additional chimeric proteins where we removed residues from PDZ3 corresponding the equivalent shorter area in PDZ1 to generate PDZ3$^{\text{PDZ1Loop–G}}$, and conversely, the corresponding three amino acids of PDZ3 residues were inserted into the PDZ1 loop to generate PDZ1$^{\text{PDZ3LoopDHS}}$ (Fig. 7). PDZ1$^{\text{PDZ3LoopDHS}}$ showed a 9-fold decrease in its affinity toward WT β-PIX peptide (32.5 μM). In contrast, PDZ3$^{\text{PDZ1Loop–G}}$ only resulted in a slight increase in affinity (9.8 μM). These data suggest that although the length of the loop is important for specificity, the residues within the loop are crucial for determining PDZ binding specificity and affinity.

Discussion

Scribble is a critical cell polarity regulator that integrates a number of signaling pathways via interactions using its four PDZ domains. Our data suggest that Scribble PDZ domains 1–4 harbor differential affinities for the PBM of β-PIX, an important guanine nucleotide exchange factor involved in cell migration and intracellular trafficking. Previous studies (22, 26) showed that Scribble PDZ1–4 domains were all able to engage β-PIX, raising the question of how specificity is achieved in this interaction and whether or not Scribble PDZ domains are able to discriminate for β-PIX binding or alternatively act in an indiscriminate manner. We now quantitatively show that Scribble PDZ1 and -3 domains are the highest affinity β-PIX binders, whereas PDZ2 displays 20-fold weaker affinity, and

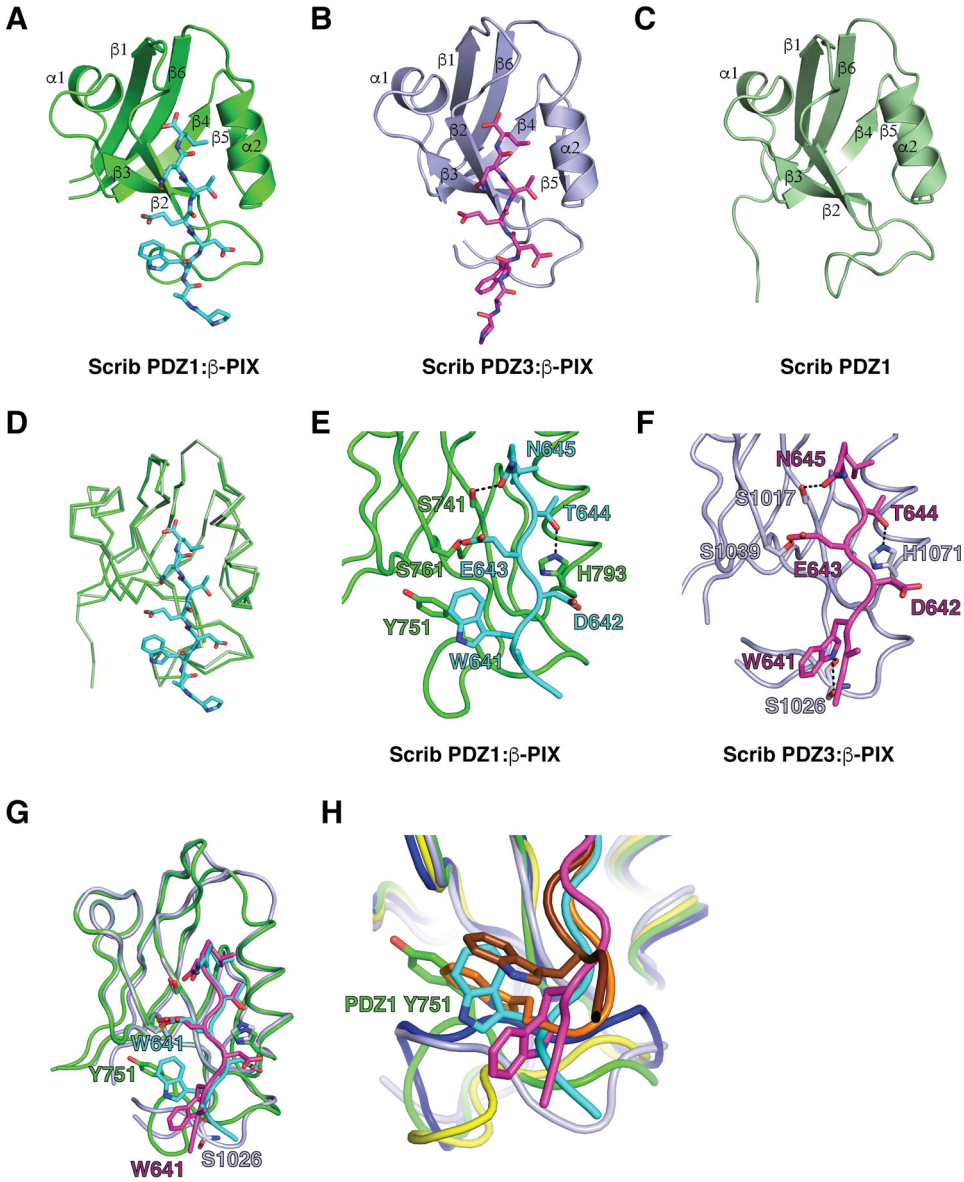

Figure 5. Crystal structures of PDZ1 and PDZ3 each bound to a β-PIX peptide. The β-PIX peptide engages individual PDZ domains via a shallow groove located between the β2 and α2. *A,* PDZ1 (*green*) is shown as a schematic with β-PIX peptide (*cyan*) represented as *sticks*. *B,* PDZ3 (*light purple*) is shown as a schematic with β-PIX peptide (*magenta*) represented as *sticks*. *C,* ligand-free PDZ1 is shown as a schematic (*forest green*). *D,* overlay of *ribbon* traces of PDZ1 with (*green*) and without β-PIX peptide (*forest green*). *E* and *F,* PDZ1 and -3 domains bound to β-PIX peptides are shown as *ribbons* and *sticks*, respectively. Side chains of the residues involved in interactions (shown as *dashed black lines*) are displayed as *sticks* and are labeled. *G,* superimposition of PDZ1 and PDZ3 bound to β-PIX peptide. *H,* superimposition of Scribble PDZ1 (*green* and *cyan*) and PDZ3 (*light purple* and *magenta*) complexes with β-PIX peptide and Erbin (*dark blue* and *chocolate*, PDB code 1N7T) and ZO-1 (*yellow* and *orange*, PDB code 2H2C) complexes with synthetic peptides.

PDZ4 is unable to interact with β-PIX (Fig. 2). Importantly, in a cellular context only, PDZ1 and -3 are able to pull down endogenous β-PIX. Overall, these findings identify Scribble PDZ1 and -3 as the primary interaction sites for β-PIX and suggest that the engagement of Scribble PDZ domains with β-PIX occurs in a highly specific manner.

At the structural level, binding of β-PIX to Scribble PDZ1 and -3 is consistent with the binding mode observed for the canonical class I PDZ domains, where side chains of Leu-0, Thr-2, Glu-3, and Trp-5 are involved in key interactions with the receiving PDZ domain. A number of the interactions with β-PIX are conserved between the PDZ1 and PDZ3 domain, including hydrogen bonds between β-PIX Asn-645 and a PDZ domain Ser, β-PIX Thr-644 and a PDZ domain His, as well as β-PIX Glu-643 and PDZ domain Ser (Fig. 5, *E*–*G*). The major difference between Scribble PDZ1 and PDZ3 binding to β-PIX centers on β-PIX Trp-641, which in PDZ1 forms hydrophobic interactions by packing against PDZ1 Gly-744 and Tyr-751, whereas in PDZ3 Trp-641 adopts a different rotamer and instead only contributes a hydrogen bond with Ser-1026, a difference that is also reflected in the ~4-fold lower affinity observed with PDZ3 and β-PIX over the PDZ1 interaction (Fig. 5*G*).

Interestingly, the β-PIX Trp at position −5 closely mimics the behavior of a key Trp at position −4 in the high affinity nanomolar Erbin complex with a synthetic high-affinity peptide (28). This Trp in position −4 has been shown to be critical for the high-affinity interaction by engaging the β2–3 loop (Fig.

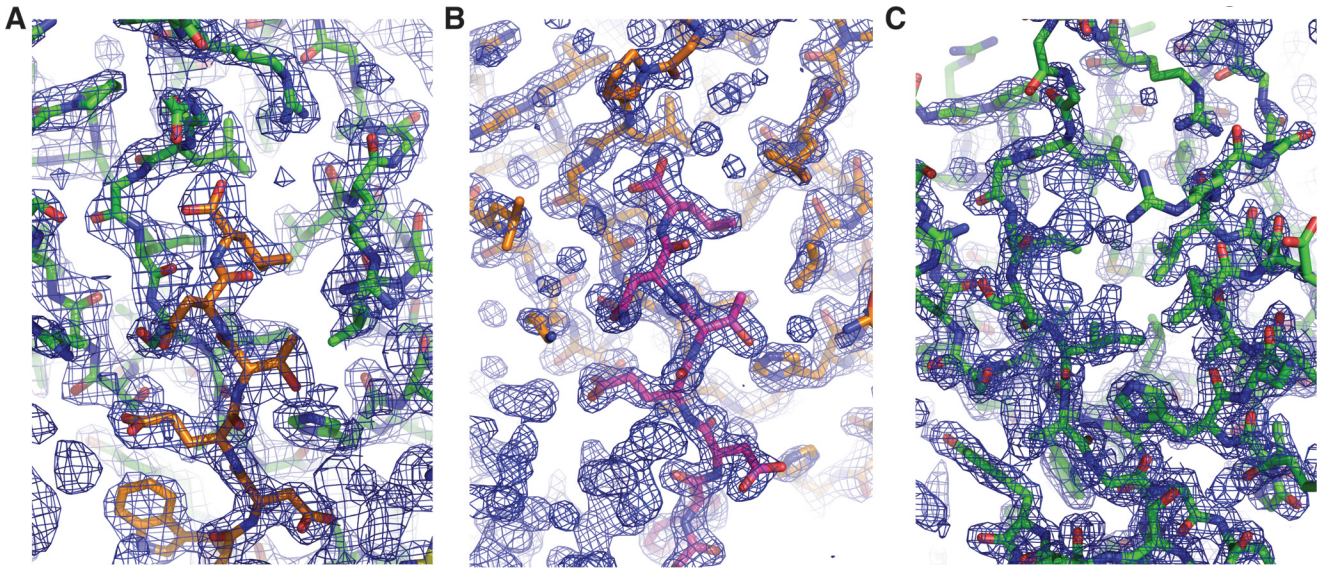

Figure 6. $2F_o - F_c$ electron density maps of PDZ1 and PDZ3 complexes with β-PIX as well as PDZ1 on its own. *A,* density map encompassing the binding groove of Scribble PDZ1 in complex with β-PIX peptide. PDZ1 is shown as *green sticks,* and β-PIX peptide is shown as *orange sticks*. The electron density map is shown as a *blue mesh* contoured at 1.5 σ. *B,* electron density map encompassing the binding groove of Scribble PDZ3 in complex with β-PIX. PDZ3 is shown as *orange sticks,* and β-PIX is shown as *magenta sticks*. The electron density map is shown as a *blue mesh* contoured at 1.5 σ. *C,* electron density map encompassing the binding groove of Scribble PDZ1 (*green sticks*). The electron density map is shown as a *blue mesh* contoured at 1.5 σ.

5*H*). Furthermore, in the high-affinity complex of ZO-1 with a different synthetic peptide (29), a Trp in the −6 position plays a similarly critical role to the Trp in the Erbin complex at position −4 by also engaging the β2–3 loop. These data suggest that the ability to form hydrophobic interactions with the β2–3 loop is an important determinant for high affinity interactions of the PDZ domain-binding ligands. Indeed, these interactions can be achieved by suitable hydrophobic residues such as Trp in the N-terminal region of the PDZ-binding motif and are not limited to a particular position, because Trp residues in the −4, −5, and −6 positions are able to engage the β2–3 loop. However, despite utilizing a Trp to contact the β2–3 loop, the affinity of the Scribble PDZ1–β-PIX interaction is an order of magnitude lower than those by Erbin and ZO-1 with synthetic peptides. In part, this can be attributed to the observation that β-PIX does not form an ionic interaction via Glu-643 with PDZ1 due to a lack of a suitable Arg residue, as observed in both Erbin and ZO-1 complexes. However, loss of the β-PIX Trp-641 hydrophobic interaction with Scribble PDZ1 Tyr-751 substantially impacts binding, with a PDZ1 Y751S mutant showing an ~8-fold lower K_D. Furthermore, the β2–3 loop also plays a critical role in controlling β-PIX binding to Scribble PDZ1 and -3 domains, because swapping of this loop between Scribble PDZ1 and -3 impairs binding of β-PIX to the resultant $PDZ1^{PDZ3LoopRegion}$ and $PDZ1^{PDZ3LoopDHS}$ chimeras, but it increases binding to the $PDZ3^{PDZ1LoopRegion}$ and $PDZ3^{PDZ1Loop-G}$ chimeras (Fig. 7). This opens the possibility of selectively engineering the length and/or identity of the residues within the PDZ β2–3 loop as shown through $PDZ1^{Y751S}$ to modulate binding to β-PIX.

A sequence alignment of all four Scribble PDZ domains reveals that key residues involved in interactions from PDZ1 to -3 with β-PIX are not fully conserved in PDZ2 and -4. In particular, the residues involved in interactions with β-PIX Trp-641 such as Tyr-751 and Ser-1026 are not found in PDZ4. Our mutagenesis data support the notion that Tyr-751 is important for binding of β-PIX, and the substitution of this residue is one of the underlying reasons for the lack of an interaction between PDZ4 and β-PIX, and possibly for the substantially lower affinity observed for PDZ2–β-PIX.

Previous studies of the shank PDZ domain interaction with β-PIX revealed that only a single β-PIX chain within the trimeric β-PIX coiled-coil engages with a shank PDZ domain at a given time (30). If a similar mechanism is involved in the PDZ domain-mediated interaction of Scribble with β-PIX, we speculate that PDZ1 is the primary interaction site for β-PIX; however, such a model awaits experimental verification.

In summary, we show that Scribble PDZ domains display differential binding affinities and capacities for binding to β-PIX and that Trp-641 of the β-PIX PBM is a key determinant for the observed differences in affinities. These findings provide a clear structural basis for Scribble–β-PIX interactions and will form the platform for detailed structure-guided investigations to understand how the differences in ability of individual PDZ domains to engage β-PIX impact the control of cell polarity and directed migration.

Experimental procedures

DNA constructs

Expression constructs encoding PDZ1, PDZ2, and PDZ4 residues 2108–2455, 2501–2896, and 3302–3616, respectively, are based on the *hScrib* transcript variant 1 (NM_182706). PDZ1t (residues 2180–2449) and PDZ3 (residues 3011–3283) and all PDZ1 and PDZ3 mutants were codon-optimized for protein expression in *Escherichia coli* BL21 (GenScript). For bacterial expression, all constructs were cloned into pGil-MBP (31) and pGex-6P-3 (GE Healthcare), except for PDZ1t, which was cloned into pGex-6P-1 (GE Healthcare).

A

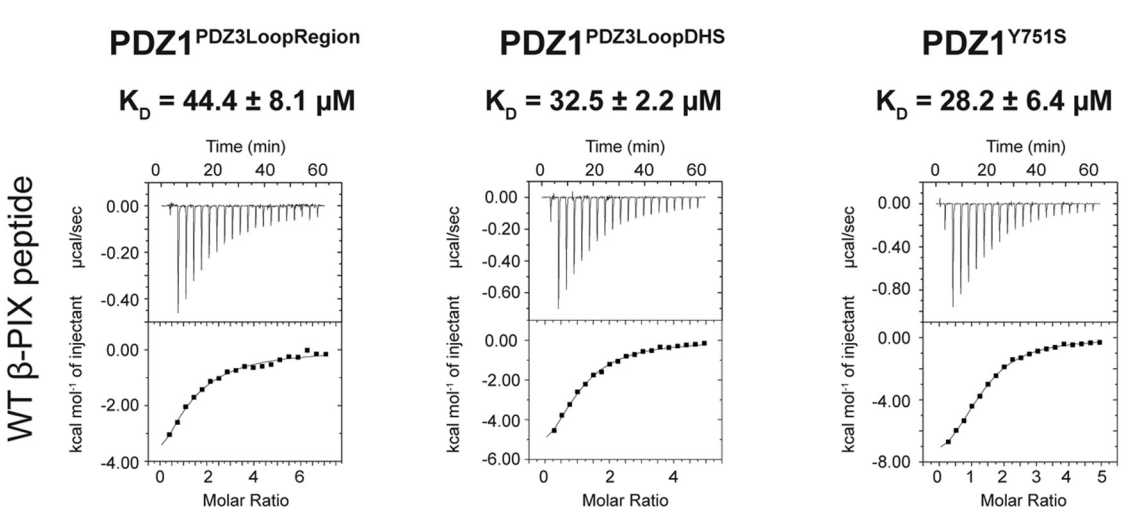

B

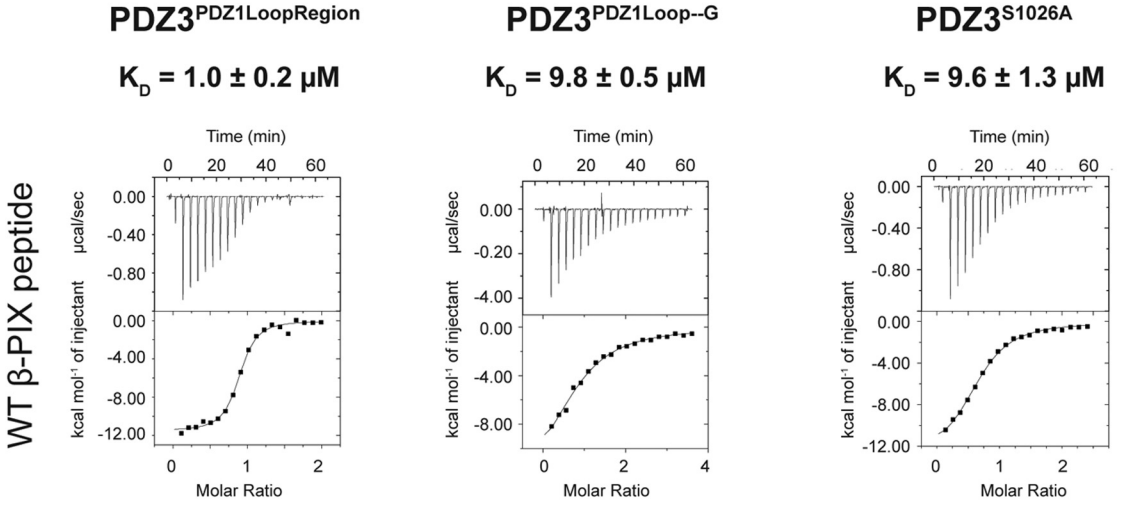

C

PROTEIN		SEQUENCE		K_D
PDZ1	737	GLGISIAGGK--GSTPYKGDDEGI	758	3.3 ± 0.3 μM
PDZ1^{PDZ3LoopRegion}	737	GLGISIAGGSDHSSHPFGVQEPGI	758	44.4 ± 8.1 μM
PDZ1^{PDZ3LoopDHS}	737	GLGISIAGGKDHSSTPYKGDDEGI	758	32.5 ± 2.2 μM
PDZ1^{Y751S}	737	GLGISIAGGK--GSTPSKGDDEGI	758	28.2 ± 6.4 μM
PDZ3	1013	PLGLSIVGGSDHSSHPFGVQEPGV	1036	14.5 ± 2.1 μM
PDZ3^{PDZ1LoopRegion}	1013	PLGLSIVGGK--GSTPYKGDDEGV	1036	1.0 ± 0.2 μM
PDZ3$^{PDZ1Loop--G}$	1013	PLGLSIVGGS--GSHPFGVQEPGV	1036	9.8 ± 0.5 μM
PDZ3^{S1026A}	1013	PLGLSIVGGSDHSAHPFGVQEPGV	1036	9.6 ± 1.3 μM

Protein expression and purification

Protein overexpression was performed using *E. coli* BL21 (DE3) pLysS cells (BIOLINE) in super broth supplemented with 200 μg/ml ampicillin (AMRESCO) using auto-induction media (10 mM Tris-Cl, pH 7.6, 100 mM NaCl, 1 mM $MgSO_4$, 0.2% (w/v) D-lactose, 0.05% (w/v) glucose, 0.5% (v/v) glycerol) (32) at 37 °C until the absorbance at 600 nm (A_{600}) reached 1.0 before transferring cultures to 16 or 25 °C for 24 h for protein expression. Proteins were also expressed via manual induction using 1 mM isopropyl 1-thio-β-D-galactopyranoside bacterial cultures at A_{600} 0.6 at 37 °C for 4 h or at 20 °C for 24 h.

Bacterial cells were harvested by centrifugation and lysed in the presence of deoxyribonuclease I (Sigma) from bovine pancreas using TS Series 0.75 kw model cabinet (Constant Systems Ltd.) at 25,000 p.s.i., Qsonica Q700 sonicator at amplitude 50 for 4 min process time on ice (5 s pulse-on time and 30 s pulse-off time) or a Fastprep®-24 (MP Biomedicals) using lysing matrix B for 20 s. Lysates were clarified by centrifugation at 20,000 × *g* for 20 min using an Avanti® J-E (Beckman Coulter). The resulting supernatant was filtered using Millex-GP syringe filter unit 0.22 μM (Merck Millipore) prior to loading onto equilibrated columns for affinity purification.

Glutathione *S*-transferase (GST)-tagged recombinant proteins were captured using glutathione-Sepharose 4B (GE Healthcare) in buffer A (50 mM Tris-Cl, pH 8.0, 150 mM NaCl, and 1 mM EDTA) and eluted with buffer A supplemented with 20 mM reduced L-glutathione. Recombinant proteins were subsequently dialyzed into buffer A to remove glutathione for the pulldown assay. GST-tagged PDZ1t was cleaved on-column with HRV 3C protease to remove the GST tag.

Hexahistidine and maltose-binding protein (His-MBP)-tagged recombinant proteins were purified using HisTrap HP columns (GE Healthcare) in buffer B (50 mM Tris-Cl, pH 8.5, 300 mM NaCl, 5 mM β-mercaptoethanol) and washed with buffer B supplemented with 20 mM imidazole before eluting in buffer B supplemented with 250 mM imidazole. His-MBP-tagged recombinant proteins were cleaved with tobacco etch virus protease in buffer B supplemented with 0.5 mM EDTA and 1 mM DTT before being subjected to a second round of affinity chromatography to remove the cleaved His-MBP tag and uncleaved fusion protein. All cleaved target proteins were subjected to size-exclusion chromatography using the HiLoad 16/600 Superdex 75 (GE Healthcare) equilibrated in 25 mM HEPES, pH 7.0, 150 mM NaCl, and eluted as a single peak.

Cell culture

Human embryonic kidneys transformed with SV40 large T antigen cell lines (HEK293T) were cultured and maintained in Dulbecco's modified Eagle's medium (DMEM) with high glucose (4500 mg/liter) (Gibco), supplemented with 20 mM HEPES, 10% fetal bovine serum (Gibco), 2 mM GlutaMAX (Gibco), 100 units/ml penicillin (Gibco), and 100 units/ml streptomycin (Gibco) at 37 °C, 5% CO_2.

GST pulldown assay

HEK293T cells were washed with Dulbecco's PBS prior to lysis with NETN lysis buffer (20 mM Tris-Cl, pH 8.0, 100 mM NaCl, 1 mM EDTA, 0.5% Nonidet P-40) supplemented with phosphatase and protease inhibitor mixture (Roche Diagnostics) for 10 min on ice. The lysate was centrifuged for 10 min at high speed using the benchtop centrifuge to remove cell debris from the sample. The protein concentration of the resulting supernatant was determined by Lowry assay using the DC™ protein assay kit (Bio-Rad). 250 μg of HEK293T supernatant was incubated with 5 μg of each GST-tagged recombinant proteins for an hour, rotating at 4 °C. 75 μl of 50% glutathione-Sepharose 4B slurry was added to each sample and incubated overnight at 4 °C. The glutathione-Sepharose 4B beads were washed three times with NETN lysis buffer before liberating the bound protein with sample loading buffer.

The samples were resolved in Bolt 4–12% BisTris Plus Gels (Invitrogen) in Bolt MOPS SDS Running buffer. Proteins were transferred to a polyvinylidene fluoride (PVDF) membrane (Millipore) via 30 V overnight at 4 °C using a Mini Trans-Blot Electrophoretic Transfer Cell (Bio-Rad).

Western blotting

All Western blottings were performed in the presence of 5% skim milk in TBS with 0.2% Tween 20. The antibodies used were rabbit polyclonal anti-β-PIX (Cell Signaling Technology), rabbit polyclonal anti-GST (Invitrogen), and secondary goat anti-rabbit IgG (Bio-Rad). Membranes were initially probed with anti-β-PIX and then stripped with stripping buffer (20 mM Tris-Cl, pH 6.8, 1% SDS, and 100 mM β-mercaptoethanol) at 60 °C for an hour for subsequent anti-GST probing. Lumi-Light enhanced chemiluminescence (Roche Diagnostics) was used to reveal the membrane.

Isothermal titration calorimetry

PDZ1 concentration was quantitated at 280 nm absorbance ($A_{280\,nm}$) using a NanoDrop 2000/2000c UV-visible spectrophotometer (Thermo Fisher Scientific). Because the concentration of PDZ2, PDZ3, and PDZ4 could not be determined by $A_{280\,nm}$, the Direct Detect® infrared spectrometer (Merck Millipore) method was used. Titrations were performed at 25 °C with a stirring speed of 1000 rpm using the MicroCal™ iTC200 system (GE Healthcare). A total of 20 injections with 2 μl each and a spacing of 180 s were titrated into the 270-μl protein sample (25 mM HEPES, pH 7.0, 150 mM NaCl), except for the first injection that was only 0.4 μl. A protein concentration of 20–100 μM against a peptide concentration of 0.5–1.4 mM was used according to the titration requirements. Peptides

Figure 7. Interaction profiles of Scribble mutant PDZ1 and -3 domains with β-PIX peptides. *A,* binding profiles of isolated mutant Scribble PDZ1 domain interactions with β-PIX peptides. Each profile is represented by a raw thermogram (*top panel*) and a binding isotherm fitted with a one-site binding model (*bottom panel*). *B,* binding profiles of isolated mutant Scribble PDZ3 domain interactions with β-PIX peptides. Each profile is represented by a raw thermogram (*top panel*) and a binding isotherm fitted with a one-site binding model (*bottom panel*). K_D, dissociation constant; ±, standard deviation; *NB,* no binding. Each of the values was calculated from at least three independent experiments. *C,* sequence details of mutant PDZ1 and PDZ3 domains used in this study. The original sequences of PDZ1 are shown in *black*, and the original sequences of PDZ3 are shown in *gray*. Mutated residues are shown as *white font* in a *black box*.

Table 1
Data collection and refinement statistics

	PDZ1–β-PIX	PDZ3–β-PIX	PDZ1
Data collection			
Space group	P 4_32_12	P 2_1	P $2_12_12_1$
No. of molecules in asymmetric units	4 + 4	2 + 2	1
Cell dimensions			
a, *b*, *c* (Å)	74.76, 74.76, 222.96	37.87, 44.16, 60.47	35.49, 41.69, 51.57
α, β, γ (°)	90.00, 90.00, 90.00	90.00, 93.61, 90.00	90.00, 90.00, 90.00
Wavelength (Å)	0.9537	0.9537	0.9537
Resolution (Å)	47.77–2.35 (2.43–2.35)	44.16–1.75 (1.78–1.75)	41.69–1.91 (1.91–1.95)
R_{sym} or R_{merge}	0.126 (0.668)	0.072 (1.759)	0.076 (0.425)
$I/\sigma I$	7.3 (1.8)	17.6 (1.0)	16.2 (4.5)
CC(1/2)	0.996 (0.738)	0.999 (0.307)	0.999 (0.856)
Completeness (%)	97.5 (99.2)	99.8 (99.9)	99.3 (95.6)
Redundancy	4.1 (4.1)	6.2 (6.1)	5.7 (5.7)
Wilson *B*-factor	26.9	24.7	20.2
Refinement			
Resolution (Å)	38.36–2.35	31.16–1.75	32.42–1.91
No. of reflections	26459	20310	6245
R_{work}/R_{free}	0.223/0.256	0.191/0.237	0.195/0.227
No. of non-hydrogen atoms			
Protein	3290	1467	1492
Ligand/ion	207	207	12
Water	263	263	48
B-Factors			
Protein	23.70	42.74	30.95
Ligand/ion	48.90	48.90	33.31
Water	33.80	33.80	30.07
r.m.s.d.			
Bond lengths (Å)	0.656	1.169	0.923
Bond angle (°)	0.004	0.011	0.008
Ramachandran plot (%)			
Favored	99.1	97.8	100
Allowed	0.9	2.2	0
Disallowed	0	0	0

were purchased from GenScript (San Francisco). The raw thermograms were processed with MicroCal Origin® version 7.0 software (OriginLab™ Corp.) to obtain the binding parameters of each interaction. Peptides used are wild-type β-PIX (NP_003890.1): ^{639}PAWDETNL^{646}, mutant β-PIX: PAWDEANA, superpeptide (27): RSWFETWV and mutant superpeptide: RSWFEAWA.

Protein crystallization

Crystallization screens were performed at the CSIRO C3 facility (Parkville, Australia) using the Phoenix Liquid Handling System (Art Robbins Instruments) as well as in-house using the Crystal Gryphon (Art Robbins Instruments). All crystals were grown at 20 °C. For PDZ1t crystals, β-PIX peptide was added to 2.92 mg/ml PDZ1t (in buffer A) with a peptide to protein ratio of 1:1.07. The final crystals were obtained in 20% (w/v) polyethylene glycol 3350, 0.2 M magnesium chloride hexahydrate. For the protein complex crystals, a protein (25 mM HEPES, pH 7.0, 150 mM NaCl) to peptide ratio of 1:5 was used for crystallization. PDZ1:β–PIX complex was prepared at a concentration of 28 mg/ml. The final crystals were obtained in 1.09 M lithium sulfate and 0.1 M trisodium citrate/citric acid, pH 5.09. PDZ3–β-PIX complex was prepared at 10 mg/ml with the final crystals being obtained in 16.6% (w/v) polyethylene glycol 3350 and 0.1 M citrate/Bistris propane, pH 8.9.

Diffraction data collection and structure determination

PDZ1t, PDZ1–β-PIX, and PDZ3–β-PIX crystals were flash-cooled in mother liquor supplemented with 20% (v/v) 2-methyl-2,4-pentanediol, 25 and 30% (v/v) ethylene glycol, respectively. All diffraction data were collected on the MX2 beamline at the Australian Synchrotron using ADSC Quantum 315r CCD detector (Area Detector Systems Corp., Poway, CA) with an oscillation range of 1.0° per frame using a wavelength of 0.9537 Å. Diffraction data were integrated using XDS (33) and scaled using AIMLESS (34, 35). The structure of the PDZ1 domain on its own as well as the complex of PDZ1–β-PIX were solved by molecular replacement using Phaser (36) with the structure of Scribble PDZ1 (PDB code 2W4F) as a search model. For PDZ1 alone, the best solution had a TFZ = 25.3 and an LLG = 699, whereas PDZ1–β-PIX had a TFZ = 59.2 and LLG = 15,288. The structure of PDZ3–β-PIX was also solved by molecular replacement using the structure of Scribble PDZ3 (PDB code 4WYT) as a search model (TFZ = 39.3 and LLG = 2216). The solutions produced by Phaser were manually rebuilt over multiple cycles using Coot (37) and refined using PHENIX (38). Data collection and refinement statistics details are summarized in Table 1. Coordinate files have been deposited in the Protein Data Bank under the accession codes 5VWC, 5VWK, and 5VWI. All images were generated using the PyMOL Molecular Graphics System, Version 1.8, Schrödinger, LLC. All software was accessed using the SBGrid suite (39). All raw diffraction images were deposited on the SBGrid Data Bank (40) using their PDB codes 5VWC, 5VWK, and 5VWI.

Author contributions—K. Y. B. L.: acquisition of data, analysis and interpretation of data, drafting and revising the article; N. J. G.: acquisition of data, analysis and interpretation of data; P. O. H.: conception and design, acquisition of data, analysis and interpretation of data, drafting and revising the article; M. K.: conception and design, acquisition of data, analysis and interpretation of data, drafting and revising the article.

Acknowledgments—We thank staff at the MX beamlines at the Australian Synchrotron for help with X-ray data collection; the CSIRO C3 Collaborative Crystallization Centre for assistance with crystallization; and the Comprehensive Proteomics Platform at La Trobe University for core instrument support.

References

1. Nelson, W. J. (2003) Adaptation of core mechanisms to generate cell polarity. *Nature* **422,** 766–774
2. McCaffrey, L. M., and Macara, I. G. (2012) Signaling pathways in cell polarity. *Cold Spring Harb. Perspect. Biol.* **4,** a009654
3. Halaoui, R., and McCaffrey, L. (2015) Rewiring cell polarity signaling in cancer. *Oncogene* **34,** 939–950
4. Humbert, P. O., Russell, S. M., Smith, L., and Richardson, H. E. (2015) in *Cell Polarity 1: Biological Role and Basic Mechanisms* (Ebnet, K., ed) pp. 65–111, Springer International Publishing, Cham, Switzerland
5. Ohno, S., Goulas, S., and Hirose, T. (2015) in *Cell Polarity 1: Biological Role and Basic Mechanisms* (Ebnet, K., ed) pp. 3–23, Springer International Publishing, Cham, Switzerland
6. Vacca, B., Barthélémy-Requin, M., Burcklé, C., Massey-Harroche, D., and Bivic, A. L. (2015) in *Cell Polarity 1: Biological Role and Basic Mechanisms* (Ebnet, K., ed) pp. 51–63, Springer International Publishing, Cham, Switzerland
7. Bilder, D., Li, M., and Perrimon, N. (2000) Cooperative regulation of cell polarity and growth by *Drosophila* tumor suppressors. *Science* **289,** 113–116
8. Zhan, L., Rosenberg, A., Bergami, K. C., Yu, M., Xuan, Z., Jaffe, A. B., Allred, C., and Muthuswamy, S. K. (2008) Deregulation of scribble promotes mammary tumorigenesis and reveals a role for cell polarity in carcinoma. *Cell* **135,** 865–878
9. Pearson, H. B., McGlinn, E., Phesse, T. J., Schlüter, H., Srikumar, A., Gödde, N. J., Woelwer, C. B., Ryan, A., Phillips, W. A., Ernst, M., Kaur, P., and Humbert, P. (2015) The polarity protein Scrib mediates epidermal development and exerts a tumor suppressive function during skin carcinogenesis. *Mol. Cancer* **14,** 169
10. Pearson, H. B., Perez-Mancera, P. A., Dow, L. E., Ryan, A., Tennstedt, P., Bogani, D., Elsum, I., Greenfield, A., Tuveson, D. A., Simon, R., and Humbert, P. O. (2011) SCRIB expression is deregulated in human prostate cancer, and its deficiency in mice promotes prostate neoplasia. *J. Clin. Invest.* **121,** 4257–4267
11. Godde, N. J., Sheridan, J. M., Smith, L. K., Pearson, H. B., Britt, K. L., Galea, R. C., Yates, L. L., Visvader, J. E., and Humbert, P. O. (2014) Scribble modulates the MAPK/Fra1 pathway to disrupt luminal and ductal integrity and suppress tumour formation in the mammary gland. *PLoS Genet.* **10,** e1004323
12. Elsum, I. A., Yates, L. L., Pearson, H. B., Phesse, T. J., Long, F., O'Donoghue, R., Ernst, M., Cullinane, C., and Humbert, P. O. (2014) Scrib heterozygosity predisposes to lung cancer and cooperates with KRas hyperactivation to accelerate lung cancer progression *in vivo*. *Oncogene* **33,** 5523–5533
13. Feigin, M. E., Akshinthala, S. D., Araki, K., Rosenberg, A. Z., Muthuswamy, L. B., Martin, B., Lehmann, B. D., Berman, H. K., Pietenpol, J. A., Cardiff, R. D., and Muthuswamy, S. K. (2014) Mislocalization of the cell polarity protein scribble promotes mammary tumorigenesis and is associated with basal breast cancer. *Cancer Res.* **74,** 3180–3194
14. Ono, Y., Urata, Y., Goto, S., Nakagawa, S., Humbert, P. O., Li, T. S., and Zammit, P. S. (2015) Muscle stem cell fate is controlled by the cell-polarity protein Scrib. *Cell Rep.* **10,** 1135–1148
15. Jarjour, A. A., Boyd, A., Dow, L. E., Holloway, R. K., Goebbels, S., Humbert, P. O., Williams, A., and ffrench-Constant, C. (2015) The polarity protein Scribble regulates myelination and remyelination in the central nervous system. *PLoS Biol.* **13,** e1002107
16. Zheng, W., Umitsu, M., Jagan, I., Tran, C. W., Ishiyama, N., BeGora, M., Araki, K., Ohashi, P. S., Ikura, M., and Muthuswamy, S. K. (2016) An interaction between Scribble and the NADPH oxidase complex controls M1 macrophage polarization and function. *Nat. Cell Biol.* **18,** 1244–1252
17. Cervantes-Sandoval, I., Chakraborty, M., MacMullen, C., and Davis, R. L. (2016) Scribble scaffolds a signalosome for active forgetting. *Neuron* **90,** 1230–1242
18. Kallay, L. M., McNickle, A., Brennwald, P. J., Hubbard, A. L., and Braiterman, L. T. (2006) Scribble associates with two polarity proteins, Lgl2 and Vangl2, via distinct molecular domains. *J. Cell. Biochem.* **99,** 647–664
19. Phua, D. C., Humbert, P. O., and Hunziker, W. (2009) Vimentin regulates scribble activity by protecting it from proteasomal degradation. *Mol. Biol. Cell* **20,** 2841–2855
20. Lahuna, O., Quellari, M., Achard, C., Nola, S., Méduri, G., Navarro, C., Vitale, N., Borg, J. P., and Misrahi, M. (2005) Thyrotropin receptor trafficking relies on the hScrib-βPIX-GIT1-ARF6 pathway. *EMBO J.* **24,** 1364–1374
21. Osmani, N., Vitale, N., Borg, J. P., and Etienne-Manneville, S. (2006) Scrib controls Cdc42 localization and activity to promote cell polarization during astrocyte migration. *Curr. Biol.* **16,** 2395–2405
22. Audebert, S., Navarro, C., Nourry, C., Chasserot-Golaz, S., Lécine, P., Bellaiche, Y., Dupont, J. L., Premont, R. T., Sempéré, C., Strub, J. M., Van Dorsselaer, A., Vitale, N., and Borg, J. P. (2004) Mammalian Scribble forms a tight complex with the βPIX exchange factor. *Curr. Biol.* **14,** 987–995
23. Dow, L. E., Kauffman, J. S., Caddy, J., Zarbalis, K., Peterson, A. S., Jane, S. M., Russell, S. M., and Humbert, P. O. (2007) The tumour-suppressor Scribble dictates cell polarity during directed epithelial migration: regulation of Rho GTPase recruitment to the leading edge. *Oncogene* **26,** 2272–2282
24. Michaelis, U. R., Chavakis, E., Kruse, C., Jungblut, B., Kaluza, D., Wandzioch, K., Manavski, Y., Heide, H., Santoni, M. J., Potente, M., Eble, J. A., Borg, J. P., and Brandes, R. P. (2013) The polarity protein Scrib is essential for directed endothelial cell migration. *Circ. Res.* **112,** 924–934
25. Nola, S., Sebbagh, M., Marchetto, S., Osmani, N., Nourry, C., Audebert, S., Navarro, C., Rachel, R., Montcouquiol, M., Sans, N., Etienne-Manneville, S., Borg, J. P., and Santoni, M. J. (2008) Scrib regulates PAK activity during the cell migration process. *Hum. Mol. Genet.* **17,** 3552–3565
26. Arnaud, C., Sebbagh, M., Nola, S., Audebert, S., Bidaut, G., Hermant, A., Gayet, O., Dusetti, N. J., Ollendorff, V., Santoni, M. J., Borg, J. P., and Lécine, P. (2009) MCC, a new interacting protein for Scrib, is required for cell migration in epithelial cells. *FEBS Lett.* **583,** 2326–2332
27. Zhang, Y., Yeh, S., Appleton, B. A., Held, H. A., Kausalya, P. J., Phua, D. C., Wong, W. L., Lasky, L. A., Wiesmann, C., Hunziker, W., and Sidhu, S. S. (2006) Convergent and divergent ligand specificity among PDZ domains of the LAP and zonula occludens (ZO) families. *J. Biol. Chem.* **281,** 22299–22311
28. Skelton, N. J., Koehler, M. F., Zobel, K., Wong, W. L., Yeh, S., Pisabarro, M. T., Yin, J. P., Lasky, L. A., and Sidhu, S. S. (2003) Origins of PDZ domain ligand specificity. Structure determination and mutagenesis of the Erbin PDZ domain. *J. Biol. Chem.* **278,** 7645–7654
29. Appleton, B. A., Zhang, Y., Wu, P., Yin, J. P., Hunziker, W., Skelton, N. J., Sidhu, S. S., and Wiesmann, C. (2006) Comparative structural analysis of the Erbin PDZ domain and the first PDZ domain of ZO-1. Insights into determinants of PDZ domain specificity. *J. Biol. Chem.* **281,** 22312–22320
30. Im, Y. J., Lee, J. H., Park, S. H., Park, S. J., Rho, S. H., Kang, G. B., Kim, E., and Eom, S. H. (2003) Crystal structure of the Shank PDZ-ligand complex reveals a class I PDZ interaction and a novel PDZ-PDZ dimerization. *J. Biol. Chem.* **278,** 48099–48104
31. Rautureau, G. J., Yabal, M., Yang, H., Huang, D. C., Kvansakul, M., and Hinds, M. G. (2012) The restricted binding repertoire of Bcl-B leaves Bim as the universal BH3-only prosurvival Bcl-2 protein antagonist. *Cell Death Dis.* **3,** e443
32. Studier, F. W. (2005) Protein production by auto-induction in high density shaking cultures. *Protein Expr. Purif.* **41,** 207–234
33. Kabsch, W. (2010) XDS. *Acta Crystallogr. D Biol. Crystallogr.* **66,** 125–132
34. Evans, P. (2006) Scaling and assessment of data quality. *Acta Crystallogr. D Biol. Crystallogr.* **62,** 72–82
35. Winn, M. D., Ballard, C. C., Cowtan, K. D., Dodson, E. J., Emsley, P., Evans, P. R., Keegan, R. M., Krissinel, E. B., Leslie, A. G., McCoy, A., McNicholas, S. J., Murshudov, G. N., Pannu, N. S., Potterton, E. A., Powell, H. R., *et al.*

(2011) Overview of the CCP4 suite and current developments. *Acta Crystallogr. D Biol. Crystallogr.* **67,** 235–242
36. McCoy, A. J. (2007) Solving structures of protein complexes by molecular replacement with Phaser. *Acta Crystallogr. D Biol. Crystallogr.* **63,** 32–41
37. Emsley, P., Lohkamp, B., Scott, W. G., and Cowtan, K. (2010) Features and development of Coot. *Acta Crystallogr. D Biol. Crystallogr.* **66,** 486–501
38. Afonine, P. V., Grosse-Kunstleve, R. W., Echols, N., Headd, J. J., Moriarty, N. W., Mustyakimov, M., Terwilliger, T. C., Urzhumtsev, A., Zwart, P. H., and Adams, P. D. (2012) Towards automated crystallographic structure refinement with phenix.refine. *Acta Crystallogr. D Biol. Crystallogr.* **68,** 352–367
39. Morin, A., Eisenbraun, B., Key, J., Sanschagrin, P. C., Timony, M. A., Ottaviano, M., and Sliz, P. (2013) Collaboration gets the most out of software. *Elife* **2,** e01456
40. Meyer, P. A., Socias, S., Key, J., Ransey, E., Tjon, E. C., Buschiazzo, A., Lei, M., Botka, C., Withrow, J., Neau, D., Rajashankar, K., Anderson, K. S., Baxter, R. H., Blacklow, S. C., Boggon, T. J., *et al.* (2016) Data publication with the structural biology data grid supports live analysis. *Nat. Commun.* **7,** 10882
41. Robert, X., and Gouet, P. (2014) Deciphering key features in protein structures with the new ENDscript server. *Nucleic Acids Res.* **42,** W320–W324